JOURNAL OF CATALYSIS **146**, 185–192 (1994)

Isobutane/2-Butene Alkylation on Ultrastable Y Zeolites: Influence of Zeolite Unit Cell Size

A. Corma,[1] A. Martínez, and C. Martínez

Instituto de Tecnología Química, UPV-CSIC, Camino de Vera s/n, 46071 Valencia, Spain

Received April 20, 1993; revised September 20, 1993

The alkylation reaction of isobutane with *trans*-2-butene has been carried out on a series of steam-dealuminated Y zeolites with unit cell sizes ranging from 2.450 to 2.426 nm. A fixed-bed reactor connected to an automatized multiloop sampling system allowed us to make differential product analysis from very short (1 min or less) to longer times on stream. A maximum in the initial 2-butene conversion was found on samples with unit cell sizes between 2.435 and 2.450 nm. However, the TMP/DMH ratio, i.e., the alkylation-to-oligomerization ratio, continuously increased with zeolite unit cell size. The concentration of reactants in the pores, the strength distribution of Brønsted acid sites, and the extent of hydrogen transfer reactions, which in turn depend on the framework Si/Al ratio of a given zeolite, were seen to affect activity and product distribution of the catalysts. Finally, the influence of these factors on the aging characteristics of the samples was also discussed. © 1994 Academic Press, Inc.

INTRODUCTION

Starting in April 1997 in the United States, emissions from gasoline and their relation to composition will be defined by the Complex Model, which has now been finalized by the U.S. Environmental Protection Agency (EPA). Model parameters for gasoline composition involve RVP, oxygenates, benzene, aromatics, olefins, ASTM T_{90}, and sulfur. In Europe and Japan, reformulation of gasoline is expected to proceed much more slowly than in the United States. Thus, in the coming years the changes to be expected in Europe are lead phase out and benzene reduction. On the other hand, after lead removal, there will be a higher demand for octane number in Europe, which, combined with a higher proportion of reformate in the total gasoline pool, will force European refiners as well to change refining strategies. Besides the ongoing increase in oxygenates, which act as octane boosters, refiners are trying to improve the octane number of the gasoline by changing the characteristics of the different gasoline streams in order to compensate the impact caused by the decrease in benzene and aromatics. In this sense, alkylation of isobutane with light olefins appears to be very attractive, since alkylate has a high MON with a low octane sensitivity (research octane–motor octane) and is a clean burning fuel provided it is mainly formed by low-reactive isoparaffins. However, the expected increase in alkylation capacity in the coming years is relatively low due to limitations imposed on the use of highly corrosive and contaminating sulfuric and hydrofluoric acids as commercial catalysts. Therefore the increased alkylation would dramatically change if the liquid acids could be replaced by new solid noncontaminant catalysts.

Much effort has been made in the last decades along this line, and zeolites have been studied as potential alkylation catalysts (1–5). Unfortunately, they have not achieved, until now, commercial application in this process because of their fast catalyst decay.

As a consequence of the successful application of Y zeolite as a cracking catalyst in the 1960s, most of the studies in the alkylation reaction (1–5) have been devoted to the use of this zeolite, either in the protonic form or exchanged with di- and/or trivalent cations. From these studies it was evidenced that the same reaction mechanism is operative when using zeolites and commercial liquid acids, although some differences in product distribution appear as a consequence of the special properties shown by zeolites, i.e., the high concentration of hydrocarbons inside the pores, and the steric limitations imposed by the molecular sieve (6). The first factor, together with the preferential adsorption of olefins versus paraffins shown by zeolites with low Si/Al ratio (7), contributes to the favoring olefin polymerization over isoparaffin–olefin alkylation, thus producing a lower quality product. Moreover, the hydrogen transfer capacity of the zeolite is of crucial importance for this reaction. As has been shown (8), most of the hydrogen transfer power of the zeolite is lost after a few minutes time on stream (TOS), and then the reaction enters a critical stage in which product distribution is better explained in terms of olefin polymerization instead of alkylation.

Both the adsorption characteristics of the zeolite (7)

---

[1] To whom correspondence should be addressed.

0021-9517/94 $6.00

and the extent of hydrogen transfer reactions (9) depend on the concentration of aluminum in the zeolite framework, or equivalently, on the unit cell size (UCS) of the Y zeolite. Nevertheless, most of the studies using Y zeolite as the alkylation catalyst were done with protonic or exchanged forms within a narrow range of Si/Al ratios. Chu and Chester (10) compared the activity of REHY, USY, REUSY, and dealuminated REHY samples with Si/Al ratios ranging from 2.6 to 4.4, but product distribution obtained with the different zeolites was not discussed. Moreover, the major part of the studies was carried out in batch or semibatch reaction systems and thus, due to the complexity of the reaction, only an averaged picture of the catalytic events occurring during the reaction could be drawn. This problem was addressed (11) by means of an experimental reaction set which combined instantaneous sampling with high-resolution product analysis.

In this work we have studied the alkylation reaction of isobutane with *trans*-2-butene on a series of steam dealuminated Y zeolites with framework Si/Al ratios ranging from 5.4 to 62.2 (UCS from 2.450 to 2.426 nm). An automated fixed-bed reactor connected to a computer-controlled multiloop sampling valve allowed us to take samples for differential analysis at very short and also at longer TOS. Then, the influence of zeolite UCS on initial activity and product distribution, and also on the aging characteristics of the catalysts, is discussed.

METHODS

Catalyst Preparation and Characterization

Four ultrastable Y zeolites (USY) with different framework compositions were supplied by PQ and were prepared from a PQ CBV-100 NaY zeolite. The dealumination was carried out by steam treatment, and samples were commercially named CBV-500, -712, -740, and -760. In this work they have been named USY-1, -2, -3, and -4. The USY-1 was obtained by calcination of sample CBV-500, which was in ammonium form, at 500°C for 3 hr. The rest of the samples were used without further treatment. From the framework and bulk Si/Al ratio, as well as from the values of surface area and crystallinity, it appears that samples CBV-712, -740, and -760 were subject to an acid treatment in order to remove extra-framework Al.

The unit cell parameter of the final samples was determined by X-ray powder diffraction using CuK_α radiation and following ASTM procedure D-3942-80. The crystallinity of the samples was calculated from the area of the (5, 3, 3) peak taking the original NaY as the reference sample. The characteristics of the resultant catalysts are given in Table 1. Before being introduced into the reactor, the zeolites were pelletized, crushed, and sieved to particle size 0.59–0.84 mm.

The acidity of the samples was measured by IR spectroscopy combined with pyridine adsorption–desorption on a Nicolet 710 FTIR spectrometer equipped with data station. For the adsorption experiments, 6.6×10^2 Pa of pyridine were introduced into the cell at room temperature. After they reached equilibrium the samples were outgassed at temperatures in the range 250–400°C under vacuum, and the spectra was recorded at room temperature. The amount of pyridine retained on the Brønsted and Lewis sites of the zeolite at the different temperatures is shown in Table 2.

Reaction System and Experimental Procedure

The alkylation reaction of isobutane (>99% purity) with *trans*-2-butene (>99% purity) has been carried out in a fixed-bed stainless-steel reactor heated by an electric furnace with three independent heating zones. The reaction system, including the feed section, reaction zone, and sampling system, was computer controlled, and it is schematized in Fig. 1. The reactants are maintained in the liquid phase in two separate vessels under nitrogen pressure and fed at the desired liquid feed rate by means of two piston-type pumps. Isobutane, 2-butene and an additional nitrogen stream of 50 cm^3/min are mixed before entering the reaction section. As can be seen in the scheme the feed mixture is by-passed at the reaction pressure, and after depressurization is analyzed until constant composition is achieved. Meanwhile, the reactor is maintained at the reaction pressure in a nitrogen atmosphere. Once the desired composition is achieved the feed mixture enters the reactor by switching the corresponding electrovalves, and it goes through the catalyst bed located in the middle zone of the reactor. The product stream coming out of the reactor is then depressurized and either condensed, if average accumulated conversions are to be obtained, or, as done in this work, diluted with a nitrogen stream of 50 cm^3/min and vaporized before going to the heated 8-loop valve sampling system. In this way samples at intervals of 1 min or less can be taken during the run and analyzed automatically once the experiment has been finished.

Reactants and products have been separated in a 100-m capillary column (fused silica, Supelco) and the individual C_1–C_8 hydrocarbons identified by means of available reference standards and GC–MS analysis. No effort has been made to identify individual C_9 and higher compounds.

The experiments reported in this work have been done using an external isobutane/2-butene molar ratio of 15 by feeding 2.13 mol/h isobutane and 0.14 mol/h 2-butene. The reaction temperature in all experiments was 50°C. In order to obtain different initial olefin conversions the WSHV, referred to 2-butene, was varied in the range 1–4 h^{-1} by changing the amount of zeolite in the reactor. Due

TABLE 1

Physicochemical Characteristics of USY Samples

Sample	Cristallinity[a] (%)	Unit cell size[a] (nm)	Si/Al framework[b]	Si/Al bulk	Crystal size (μm)	Surface area[c] (m^2/g)	%Na_2O (wt%)
CBV-100	100	2.467	2.6	2.6	0.4–0.6	900	Na_2O/Al_2O_3 = 1.02
USY-1	60	2.450	5.4	2.6	—	750	0.18
USY-2	83	2.435	13.6	5.8	—	730	0.05
USY-3	91	2.428	35.3	21.0	—	750	0.03
USY-4	46	2.426	62.2	28.0	—	720	0.03

[a] From XRD data.

[b] Calculated from the Fichtner–Schmittler equation (12).

[c] $p/p_0 = 0.03$.

to the exothermicity of the reaction the zeolite was diluted with inert silica (50/50 by weight). Before being reused, the catalysts were regenerated by calcination in a flow of air at 500°C for 10 h.

RESULTS AND DISCUSSION

Initial Activity and Selectivity

As said above, the major drawback of zeolites as alkylation catalysts is catalyst deactivation, which occurs after a few minutes TOS (8, 11). This probably occurs as a consequence of acid site poisoning, and pore blockage by large molecules formed mainly by polymerization reactions. This fast decay makes it quite difficult to compare the intrinsic activity of different catalysts, especially when batch or semibatch reactors are used. The problem can be overcome by comparing the activity of the catalysts under the same experimental conditions, at 1 min TOS, and hence in the absence of deactivation. In this way, when the 2-butene conversion obtained at 1 min TOS is plotted versus the unit cell size of the different USY samples (Fig. 2) a maximum is observed at 2.435–2.445 nm UCS (13.6–7.0 Si/Al ratio). For samples with UCS below 2.435 nm a strong decrease in the olefin conversion occurs, while in the case of UCS above 2.445 nm the decrease in conversion is much less pronounced. From these results and taking into account the distribution of the different acid sites that can be present in Y zeolites, assuming a random aluminum distribution in the framework (13), it can be concluded that strong acid sites, i.e., those associated with aluminum having 0 and 1 Al in next nearest neighbors (NNN) positions, are responsible for the alkylation reaction.

However, the above argument can lead to misleading conclusions, as the 2-butene conversion cannot be taken as a measure of the intrinsic activity of the zeolite for the alkylation reaction, since oligomerization of the olefin also occurs. The extent of the two competing reactions can be calculated from the yield of the different reaction products. Indeed, trimethylpentanes (TMP) are the primary products formed by direct addition of isobutane to 2-butene (Eq. [1]), while dimethylhexanes (DMH) are mainly formed from the olefin by dimerization reactions

TABLE 2

Acidity of USY Samples as Measured by IR Pyridine Adsorption and Desorption at Different Temperatures

	Acidity (μmol Py/g catalyst)[a]						
	Brønsted			Lewis			Ratio of $(400/250)_B$ acid sites
Sample	250°C	350°C	400°C	250°C	350°C	400°C	
USY-1	110	58	28	41	34	27	0.25
USY-2	80	32	13	29	18	14	0.16
USY-3	46	18	4	16	10	7	0.08
USY-4	39	15	2	20	14	13	0.05

[a] Calculated using the extinction coefficients given elsewhere (17).

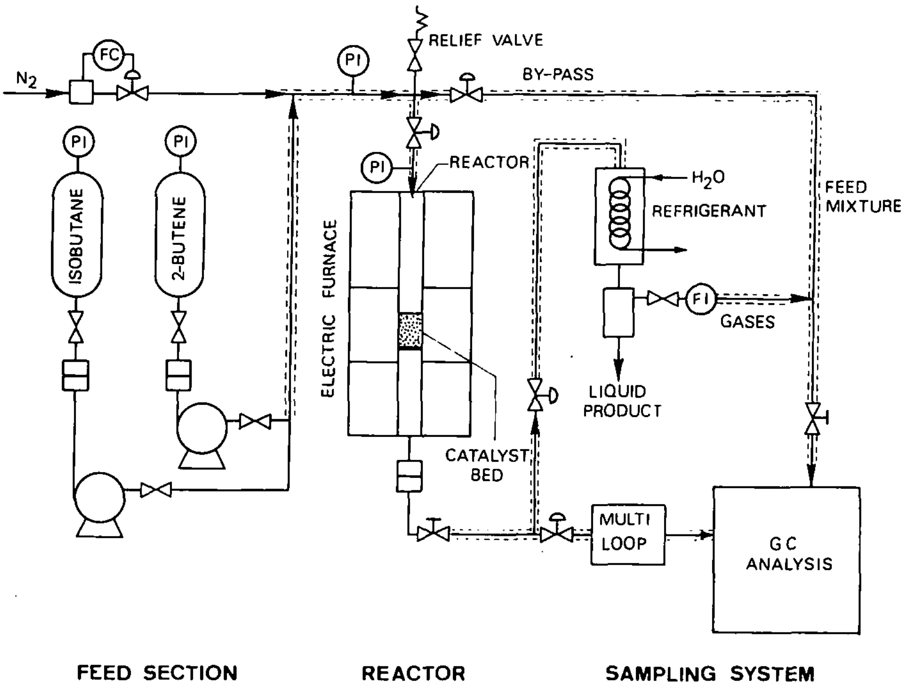

FIG. 1. Schematic representation of the experimental reaction system.

(Eq. [2]). Cracking of larger carbocations can also lead to the formation of some TMP and DMH according to Eq. [3]:

$$t\text{-}C_4^+ + 2 - C_4^= \rightarrow 2,2,3\text{-TMP}^+ \quad [1]$$

$$\text{sec-}C_4^+ + 2 - C_4^= \rightarrow 3,4\text{-DMH}^+ \quad [2]$$

$$\text{i-}C_{16}^+ \rightarrow \text{DMH}^+ + \text{TMP}^+. \quad [3]$$

Then, the TMP/DMH ratio can be taken, in principle, as a measure of the alkylation-versus-oligomerization ability of the zeolite. When this is done for the different USY samples (Fig. 3) a continuous increase of the alkylation-to-oligomerization ratio is observed when decreasing the framework Si/Al ratio, up to 5.4. In a first approximation, and considering a topological model of Al distribution in Y zeolite, these results may suggest that, contrary to what is commonly believed, isobutane alkylation in zeolites does not necessarily require very strong acid sites, but probably what becomes more important is

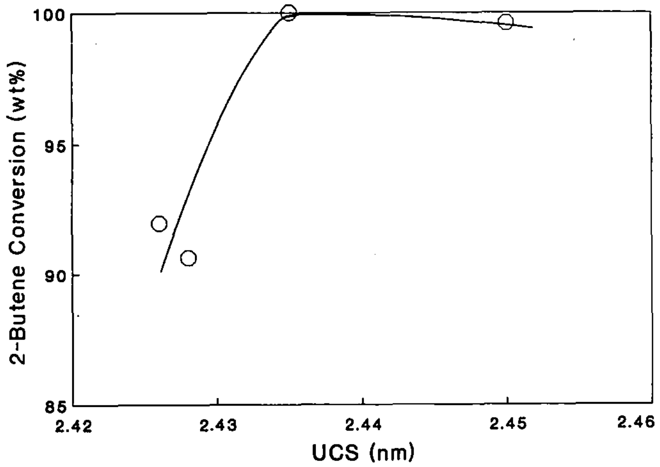

FIG. 2. 2-Butene conversion obtained at TOS = 1 min as a function of the unit cell size of USY samples.

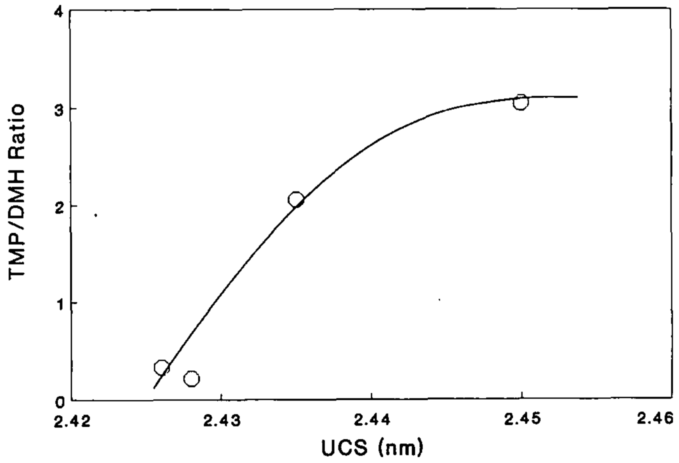

FIG. 3. TMP/DMH ratio at 1 min TOS as a function of the unit cell size of USY samples.

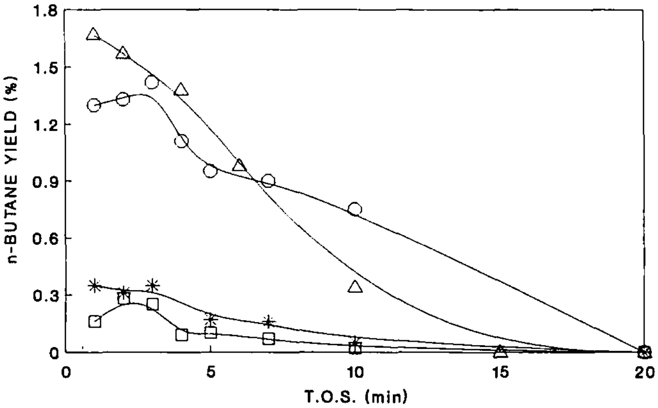

FIG. 4. Formation of *n*-butane during the alkylation reaction of isobutane with 2-butene on (○) USY-1, (△) USY-2, (□) USY-3, and (*) USY-4 samples.

achieving a high concentration of reactants in the zeolite pores. This in turn can support Kirsch *et al.*'s (3) assumption that only some Si–O–R hydrocarbon/zeolite complexes can be considered as alkylation precursors. Thus, the higher the concentration of reactants in the pores, the higher the number of alkylation precursors should be, which would explain the increase in the alkylation capacity of the zeolite when increasing the UCS.

There is, however, another important factor which has to be considered in order to discuss activity, selectivity, and also catalyst decay on zeolite alkylation catalysts: the ability of the zeolite to catalyze hydrogen transfer reactions. Indeed, when a *tert*-butyl cation has alkylated a butene molecule, the C_8 carbenium ion formed has to be rapidly desorbed before it may undergo consecutive reactions leading to high molecular weight products, which are difficult to desorb. Thus, one way to increase the number of the desired t-C_4^+ alkylating species, and to decrease the average life time of the adsorbed C_8 carbenium ions while keeping the reaction chain transfer, is by increasing the rate of hydrogen transfer from isobutane. It is well known (9) that when decreasing the unit cell size of the Y zeolite below ca. 2.430 nm a strong decrease of the hydrogen transfer activity occurs.

The effect of hydrogen transfer during alkylation is directly seen in Fig. 4, where the yield of *n*-butane, defined as grams of *n*-butane formed per gram of 2-butene fed, has been represented as a function of TOS for the four USY samples. According to the accepted reaction mechanism (11, 15, 16), the initial step of the reaction chain is protonation of the olefin followed by hydrogen transfer from isobutane giving a *t*-butyl cation and an *n*-butane molecule (Eq. [4]). Then, the amount of *n*-butane formed at the initial reaction stages will be indicative of the hydrogen transfer activity of the catalyst. Results from Fig. 4 show that the amount of *n*-butane in the first minutes of reaction is higher for the samples with higher UCS. The low rate of *t*-butyl carbenium ion production on the low UCS zeolites, as evidenced by their low *n*-butane production at the early stages of the reaction, will also determine the lower alkylation activity observed. Consequently, conjunctive polymerization, rather than alkylation, is favored on the low UCS samples:

$$\text{sec-}C_4^+ + \text{i-}C_4 \rightarrow n\text{-}C_4 + t\text{-}C_4^+. \qquad [4]$$

This can also be deduced from the product distribution of the alkylate obtained at 1 min TOS on the different USY samples, which is presented in Tables 3 and 4. There it can be seen that the amount of cracked products, C_5–C_7 hydrocarbons, is higher on the samples with UCS above 2.430 nm as a consequence of their higher cracking activity with respect to the lower UCS samples. On the other hand, the later produced a higher amount of C_{9+} hydrocarbons which are formed by consecutive condensation reactions as a consequence of the lower rate of desorption of

TABLE 3

Alkylate Product Distribution (TOS = 1 min) for USY Samples with Different Unit Cell Sizes

Zeolite UCS (nm)	2.450	2.435	2.428	2.426
2-Butene conversion (wt%)	99.60	100.00	90.63	91.96
Alkylate yield (g C_{5+}/g olefin charged)	0.84	0.48	0.19	0.20
Product distribution (wt%)				
C_5–C_7				
i-P	15.031	15.649	3.803	4.879
2,3-DMB	6.132	5.651	1.076	1.433
2-MP	1.762	1.698	0.850	1.135
3-MP	2.028	2.219	1.676	2.064
C_6 olefins	0.000	0.000	0.156	0.171
2,4-DMP	4.674	3.518	0.460	0.606
2,2,3-TMB	0.357	0.366	0.148	0.171
2-MH	0.450	0.273	0.164	0.196
2,3-DMP	2.943	2.908	1.567	1.629
3-MH	0.577	0.524	0.787	0.904
C_7 olefins	0.038	0.000	0.140	0.128
Total	33.992	32.805	10.826	13.316
C_8				
2,2,4-TMP	14.736	11.384	1.317	1.894
2,5-DMH	1.204	0.722	0.156	0.179
2,2,3-TMP + 2,4-DMH	5.625	3.669	2.120	2.201
2,3,4-TMP	8.617	7.984	2.151	2.602
2,3,3-TMP	11.628	8.200	1.317	1.604
2,3-DMH	3.468	4.491	9.235	8.146
3,4-DMH	2.544	4.304	16.834	12.420
C_8 olefins	0.826	0.144	16.172	10.517
Total	48.649	52.367	49.302	39.563
TMP/DMH ratio	3.78	2.58	0.21	0.33
C_{9+}	17.359	23.100	39.872	47.121

TABLE 4

Comparison of Product Selectivity at 91 wt% Olefin Conversion Level for the Different USY Samples (TOS = 1 min)

Sample	USY-1	USY-2	USY-3	USY-4
Composition of C_{5+} (wt%)				
C_5–C_7	24.0	19.2	10.9	13.3
C_8	59.5	54.4	49.3	39.6
C_{9+}	16.5	26.4	39.8	47.1
Composition of C_8's (wt%)				
TMP	70.0	63.0	11.9	18.2
DMH	23.1	30.6	55.3	55.2
Olefins	6.9	6.4	32.8	26.6
TMP/DMH Ratio	3.03	2.06	0.22	0.22
Composition of TMPs (wt%)				
2,2,4-TMP	34.2	32.9	22.6	26.3
2,2,3-TMP	7.4	6.3	18.1	15.3
2,3,4-TMP	28.3	31.6	36.8	36.2
2,3,3-TMP	30.1	29.2	22.5	22.2

C_8 carbocations due to the lower hydrogen transfer activity.

In regard to the distribution of the individual C_8 isomers it can be seen that with the high UCS zeolites the amount of TMP exceeds that of DMH. Furthermore, the 2,2,4-TMP is the predominant isomer formed at this initial reaction stage on these samples, while 2,2,3-TMP, which should be the primary product from isobutane and 2-butene (Eq. [1]), is formed to a much lesser extent. The distribution of TMP isomers observed can be explained by considering that there is a rapid isomerization of the trimethylpentyl cations on the zeolite acid sites. Nevertheless, formation of 2,2,4-TMP from the so-called isobutane self-alkylation (Eqs. [5] and [6]) has been shown to occur extensively when zeolites are used as alkylation catalysts (2, 3):

$$t\text{-}C_4^+ \rightarrow i\text{-}C_4^= + H^+ \qquad [5]$$

$$t\text{-}C_4^+ + i\text{-}C_4^= \rightarrow 2,2,4\text{-}TMP^+. \qquad [6]$$

Dimethylhexanes are the predominant compounds of the C_8 fraction formed on the lower UCS samples at the initial reaction stages. Among these, the 3,4-DMH is present in a greater concentration. This clearly indicates that on these samples the reaction pathway goes preferentially through olefin dimerization (Eq. [2]) instead of isoparaffin/olefin alkylation. Moreover, a considerable amount of isooctenes, about 30 wt% of the C_8 fraction, appears in the product as a consequence of the lower hydrogen transfer activity shown by the lower UCS zeolites. Indeed, when the hydrogen transfer activity is low the desorption of the carbocations from the acid sites should occur by giving back a proton to the catalyst while forming the corresponding olefin:

$$i\text{-}C_8^+ + O^-\text{-Zeol} \rightarrow H\text{-}O\text{-Zeol} + i\text{-}C_8^=. \qquad [7]$$

At this point it appears that the alkylation–olimerization properties of a given zeolite are determined by zeolite factors such as density of acid sites, electric fields which control the concentration of reactants in the pores, and hydrogen transfer ability. However, these factors cannot be separated from others related to the total number and strength of the acid sites, and it is therefore convenient to also look into the possible role of acidity in USY samples. In this way, results from Table 2 show that the total amount of strong acid sites, i.e., those retaining pyridine at 400°C, increases in the order USY-1 > USY-2 > USY-3 > USY-4. This is the same order which has been observed for the activity of the catalysts to produce TMP, i.e., for the alkylation of isobutane with 2-butene (Fig. 3). Then, it could be said, in principle, that the higher the concentration of strong acid sites, the higher the alkylation activity would be. Nevertheless, the strength of acid sites in HY zeolites is lower than those of concentrated sulfuric or HF acids. Therefore, it appears that the fact that zeolites concentrate reactants in the cavities has an important effect on the high alkylation rate observed on these catalysts. Furthermore, the proportion of the strong to strong-plus-medium strength acid sites, given by the ratio of the pyridine remaining adsorbed after 400 and 250°C desorption temperature, decreases in the order USY-1 > USY-2 > USY-3 > USY-4 (Table 2). Thus, since results from Fig. 3 do indicate that the ratio of alkylation to oligomerization decreases when decreasing the unit cell size, one may also conclude that olefin oligomerization can be carried out on acid sites weaker than alkylation. If this is so, in order to maximize alkylation, it would be desirable to have in a zeolite with a given hydrogen transfer hability a high ratio of stronger to weaker acid sites.

So far, it is possible to say that in order to design active and selective zeolite-based alkylation catalysts one has to achieve a high concentration of reactants, especially isobutane, within the zeolite pores, a high concentration of strong acid sites, and a high hydrogen transfer activity.

Catalyst Deactivation and Product Distribution with TOS

The activity and selectivity obtained in the absence of deactivation were seen to depend on the concentration of reactants in the pores, nature of Brønsted acid sites, and zeolite hydrogen transfer activity. Then, the framework Si/Al ratio of the zeolite, which controls all the above factors, is also expected to affect the aging characteristics of the catalysts.

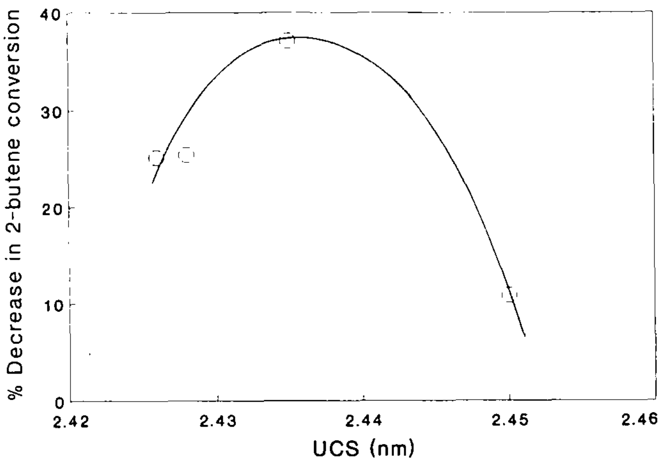

FIG. 5. Decrease in 2-butene conversion after 10 min TOS versus the UCS of USY samples.

If referred to the total 2-butene conversion, the fraction of activity lost after a reaction time of 10 min was maximum for sample USY-2 with unit cell size of 2.435 nm (Fig. 5). This sample was seen to give the highest 2-butene conversion at the first minute TOS. In the first part of the work we concluded that the strongest Brønsted acid sites were the responsible for the alkylation reaction (formation of TMP), while olefin dimerization (formation of DMH) mainly occurred on the weakest sites. Then, in order to differentiate the deactivation on both type of sites, the fraction of the initial TMP and DMH lost after a reaction time of 10 min has been represented as a function of the zeolite UCS (Fig. 6). It can be observed in this figure that the rate of decrease of TMP is always higher than that of DMH, irrespective of the UCS of the zeolite. These results suggest that the stronger Brønsted acid sites, which form TMP from alkylation, deactivate faster than those active for olefin dimerization. Moreover, if deactivation occurs by formation of heavy hydrocarbons remaining adsorbed on the zeolite acid sites, then the rate of hydrogen transfer reactions which controls the rate of desorption of carbocations from the acid sites, and can limit the

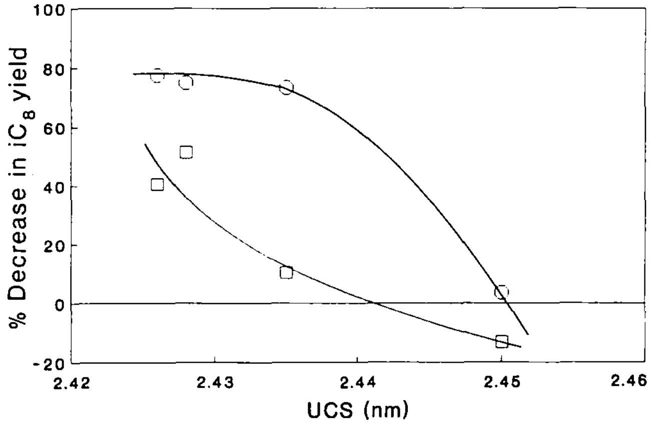

FIG. 6. Decrease in TMP (O) and DMH (□) yield after 10 min TOS as a function of the UCS of USY samples.

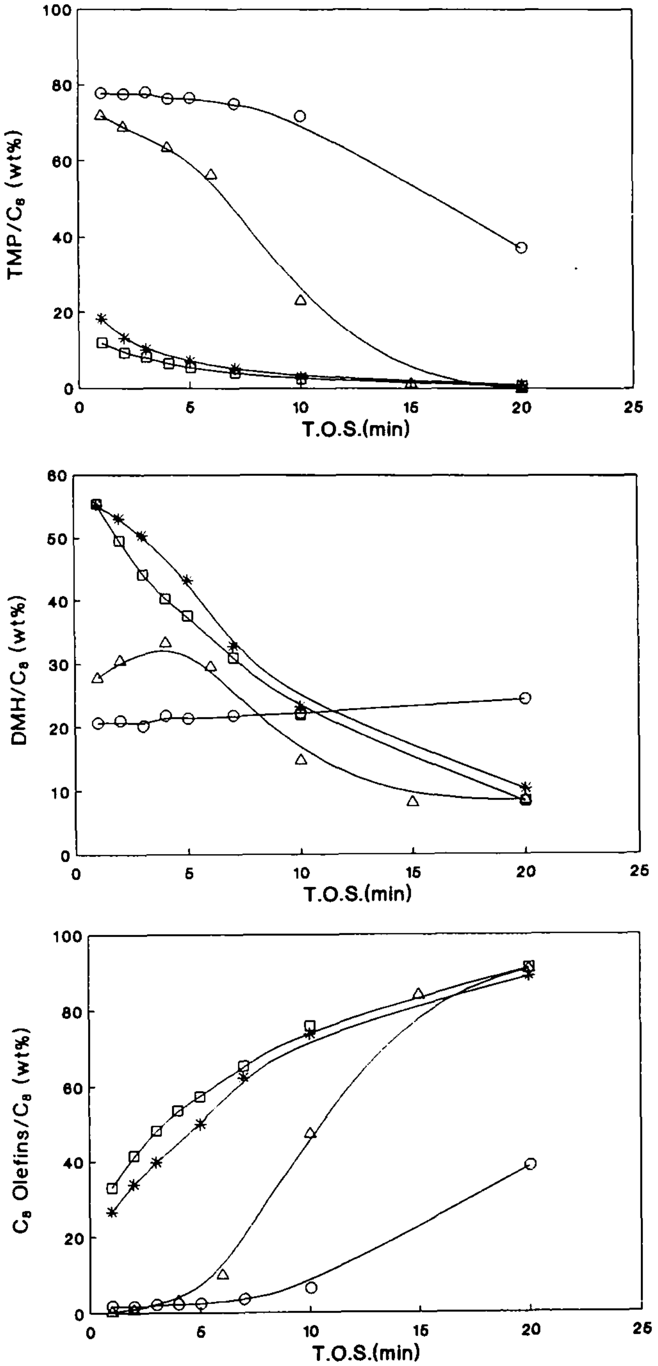

FIG. 7. Change in composition of the C_8 fraction during alkylation for the different USY samples: (O) USY-1, (△) USY-2, (□) USY-3, and (*) USY-4.

molecular weight of the final product molecule, should play an important role in catalyst decay.

Indeed, as the reaction proceeds and hydrogen transfer is more and more lost, the amount of condensed products increases and 2-butene conversion strongly decreases. Moreover, the olefinicity of the product rises, as desorption of the carbenium ions now occurs by restoring the proton to the catalyst while forming the corresponding olefin. This can be observed in Fig. 7, where the composition of the C_8 fraction of the product has been represented as a function of time on stream.

CONCLUSIONS

A continuous increase of the TMP/DMH ratio, i.e., the alkylation-to-oligomerization ratio, with increasing zeolite UCS has been observed. This behavior was seen to correlate with the activity of the zeolite to catalyze hydrogen transfer reactions, and with the ratio of stronger to weaker Brønsted acid sites. Thus, as olefin dimerization preferentially occurs on the weaker sites, a high ratio of stronger to weaker acid sites is needed if one wants to obtain high alkylation activity while avoiding olefin dimerization.

Dimethylhexanes are the predominant compounds formed on the low UCS zeolites at the initial reaction stages, 3,4-DMH being the majority isomer. This indicates that on these samples, with very low concentration of strong Brønsted acid sites and low hydrogen transfer activity, the product distribution is explained in terms of olefin dimerization. By contrast, high UCS zeolites yield a high concentration of TMP with a high ratio of 2,2,4-/2,2,3-TMP isomers. This was explained by rapid isomerization of the C_8 carbenium ions on the zeolite acid sites, together with isobutane self-alkylation.

At the initial stages of the reaction, hydrogen transfer increases with zeolite UCS, and so does the *n*-butane formed. A high hydrogen transfer activity decreases the average lifetime of the carbocations on the zeolite acid sites, thus decreasing the probability of undergoing secondary reactions. Low UCS zeolites, which are poor catalysts for hydrogen transfer reactions, yield a reasonable amount of isooctenes at the initial reaction stages.

Deactivation of the stronger Brønsted acid sites was seen to occur faster than that of the weaker sites, irrespective of the UCS of the zeolite. However, the relative rate of decrease in TMP formation depended on both the concentration of strong acid sites and the rate of decrease in hydrogen transfer activity of the zeolite. This in turn depended on the framework Si/Al ratio of the zeolite.

The decrease in hydrogen transfer reactions as the zeolite ages is responsible for an increase of the olefinic content in the C_8 products, which is accompanied by a decrease in 2-butene conversion.

ACKNOWLEDGMENT

Financial support by the Dirección General de Investigación Científica y Técnica of Spain (Project MAT 91-1152) is gratefully acknowledged.

REFERENCES

1. Kirsch, F. W., and Potts, J. D., *Prepr. Am. Chem. Soc. Div. Pet. Chem.* **15** (3), A-109 (1970).
2. Kirsch, F. W., Lauer, J. L., and Potts, *Prepr. Am. Chem. Soc. Div. Pet. Chem.*, B24 (1971).
3. Kirsch, F. W., Potts, J. D., and Barmby, D. S., *J. Catal.* **27**, 142 (1972).
4. Huang, T. J., and Yurchak, S., *ACS Symp. Ser.* **55**, 75 (1977).
5. Minachev, K. M., Mortinov, E. S., Zen'kovski, S. M., Mostovoy, N. V., and Kononov, N. F., *ACS Symp. Ser.* **55**, 89 (1977).
6. Corma, A., and Martínez, A., *Catal. Rev. Sci. Eng.* **35**(4), 483 (1993).
7. Corma, A., Faraldos, M., Martínez, A., and Mifsud, A., *J. Catal.* **122**, 230 (1990).
8. Weitkamp, J., *in* "Proceedings, 5th International Conference Zeolites" (L. Rees, Ed.), p. 858. Wiley, New York, 1980.
9. Pine, L., Maher, P.J., and Watcher, W. A., *J. Catal.* **85**, 466 (1984).
10. Chu, Y. F., and Chester, A. W., *Zeolites* **6**, 195 (1986).
11. Weitkamp, J., *in* "Catalysis by Zeolites: Proceedings" (B. Imelik *et al.*, Eds.), Studies in Surface Science and Catalysis, Vol. 5, p. 65. Elsevier, Amsterdam, 1980.
12. Fichtner-Schmitler, H., Lose, R., Engelhardt, G., and Patzelova, V., *Cryst. Res. Technol.* **19**, k1 (1984).
13. Beagley, B., Dwyer, J., Fitch, F. R., Mann, R., and Walters, J., *J. Phys. Chem.* **88**, 1744 (1984).
14. Corma, A., Fornés, V., Martínez, A., and Orchillés, A. V., *ACS Symp. Ser.* **368**, 542 (1988).
15. Lerno, H., and Citarella, V. A., *Hydrocarbon Process.* **Nov.** (1991).
16. Kovalinka, J. A., Sholten, J. J., and Rasser, J. C., *J. Catal.* **48**, 365 (1977).
17. Hughes, T. R., and White, H. M., *J. Phys. Chem.* **71**, 2192 (1967).